Earth's Future

Corresponding author:
K. G. Miller, kgm@rci.rutgers.edu

A geological perspective on sea-level rise and its impacts along the U.S. mid-Atlantic coast

Kenneth G. Miller[1,2], Robert E. Kopp[1,2,3], Benjamin P. Horton[2,4], James V. Browning[1], and Andrew C. Kemp[5]

[1]Department of Earth and Planetary Sciences, Rutgers University, Piscataway, New Jersey, USA, [2]Institute of Marine and Coastal Sciences, Rutgers University, New Brunswick, New Jersey, USA, [3]Rutgers Energy Institute, Rutgers University, New Brunswick, New Jersey, USA, [4]Division of Earth Sciences and Earth Observatory of Singapore, Nanyang Technological University, Singapore, Singapore, [5]Department of Earth and Ocean Sciences, Tufts University, Medford, Massachusetts, USA

Abstract We evaluate paleo-, historical, and future sea-level rise along the U.S. mid-Atlantic coast. The rate of relative sea-level rise in New Jersey decreased from 3.5 ± 1.0 mm/yr at 7.5–6.5 ka, to 2.2 ± 0.8 mm/yr at 5.5–4.5 ka to a minimum of 0.9 ± 0.4 mm/yr at 3.3–2.3 ka. Relative sea level rose at a rate of 1.6 ± 0.1 mm/yr from 2.2 to 1.2 ka (750 Common Era [CE]) and 1.4 ± 0.1 mm/yr from 800 to 1800 CE. Geological and tide-gauge data show that sea-level rise was more rapid throughout the region since the Industrial Revolution (19th century = 2.7 ± 0.4 mm/yr; 20th century = 3.8 ± 0.2 mm/yr). There is a 95% probability that the 20th century rate of sea-level rise was faster than it was in any century in the last 4.3 kyr. These records reflect global rise ($\sim 1.7 \pm 0.2$ mm/yr since 1880 CE) and subsidence from glacio-isostatic adjustment ($\sim 1.3 \pm 0.4$ mm/yr) at bedrock locations (e.g., New York City). At coastal plain locations, the rate of rise is 0.3–1.3 mm/yr higher due to groundwater withdrawal and compaction. We construct 21st century relative sea-level rise scenarios including global, regional, and local processes. We project a 22 cm rise at bedrock locations by 2030 (central scenario; low- and high-end scenarios range of 16–38 cm), 40 cm by 2050 (range 28–65 cm), and 96 cm by 2100 (range 66–168 cm), with coastal plain locations having higher rises (3, 5–6, and 10–12 cm higher, respectively). By 2050 CE in the central scenario, a storm with a 10 year recurrence interval will exceed all historic storms at Atlantic City.

Summary An analysis of geological and historical sea-level records shows a significant rate of increase in sea-level rise since the nineteenth century. In New Jersey, it is extremely likely that sea-level rise in the twentieth century was faster than during any other century in the last 4.3 thousand years. Accounting for regional and local factors, the authors project sea-level rise in the mid-Atlantic U.S. most likely about 38–42'' (96–106 cm) over the twentieth century, but possibly as high as 66–71'' (168–180 cm).

1. Introduction

Anthropogenic, climatically driven sea-level rise occurs in the context of geologically driven sea-level changes. An understanding of both anthropogenic and natural drivers is necessary to plan for coastal adaptation. As a case study, we evaluate past, present, and future relative sea-level changes on the U.S. mid-Atlantic coast (New York to Virginia; Figure 1), providing insight into interactions among global average sea-level rise, subsidence induced by regional (thermoflexural and isostatic) and local (compaction) effects, and oceanographic (changes in dynamic height) processes. The U.S. mid-Atlantic region is the most densely populated in the United States, with about 40 million residents in the metropolitan areas between New York City and Washington, D.C. [*U.S. Census Bureau*, 2013]. The region is impacted by flooding due to tropical storms and extra-tropical cyclones (nor'easters), compounded by sea-level rise. Flooding achieved during a storm (storm tide) is the result of storm-surge height plus the timing in the astronomical tidal cycle, but storm flooding is added on to slowly rising relative sea level. The mid-Atlantic U.S. region has been identified as a "hot spot" for sea-level rise [*Sallenger et al.*, 2012], with a sharp acceleration noted in some tide-gauge records [*Kemp et al.*, 2009; *Boon*, 2012; *Ezer and Corlett*, 2012; *Kopp*, 2013].

Superstorm Sandy made landfall on 30 October 2012 as one of the strongest storms to batter the U.S. mid-Atlantic coast (Figure 1), with damage primarily due to severe flooding. The storm tide from Sandy was unprecedented at the Battery tide gauge in New York City at 4.26 m above mean lower low water
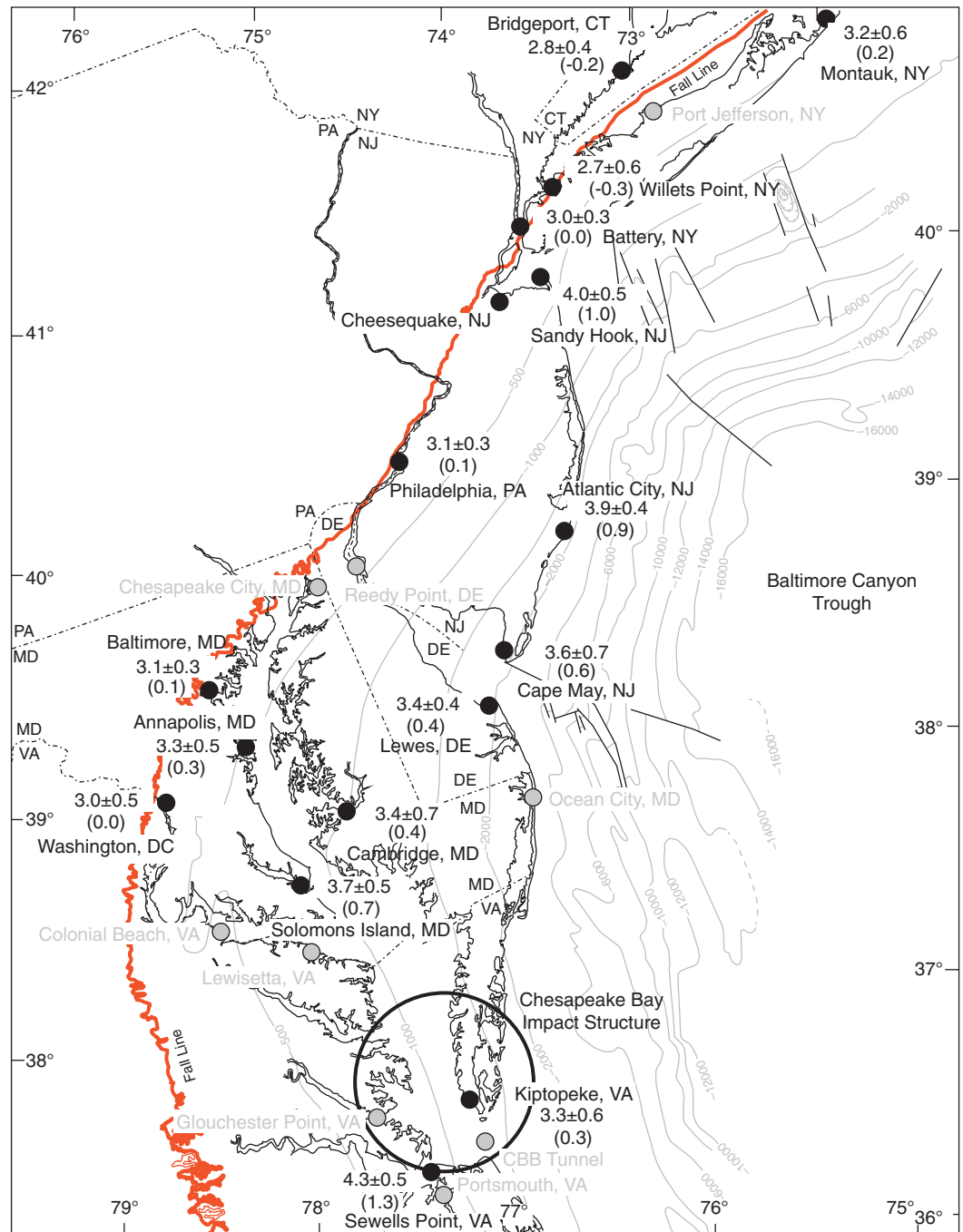
Figure 1. Relative sea-level rise and sea-level anomaly from tide-gauge data superimposed on geological map of *Benson* [1984]. Plotted are the linear trends from *Kopp* [2013] from 1900 and the subsidence anomaly derived by subtracting the trend at the Battery. Structural contours on the coastal plain and the Baltimore Canyon Trough are to basement in meters. Gray circles are tide gauges with insufficient length (<60 yr.). Red = Fall Line.

[MLLW; we refer to MLLW because this reference frame is used by the U.S. Federal Emergency Management Agency (FEMA) for coastal flood elevations] compared to the previous peak of 3.05 m during Hurricane Donna in 1960 [*Kemp and Horton*, 2013]. However, storm tides are moving markers that are exacerbated by sea-level rise. A largely anthropogenically driven global sea-level (GSL) rise of 20 cm during the 20th century [*Church and White*, 2011] caused Sandy to flood an area ~70 km² greater than it would have in 1880, increasing the number of people living on land lower than the storm tide by ~38,000 in New Jersey and by ~45,000 in New York City (Climate Central, Surging Seas Data Table, 2012, retrieved

from SurgingSeas.org/downloadables, based on methodology from SurgingSeas.org/NationalReport, last updated February 2012).

Temperature and ice-volume variations control global average sea-level changes on the 10^5 year to multiannual scale [*Miller et al.*, 2005], with the geological record testifying to rapid periods of rise. During the last deglaciation (∼20–9 ka), mean rates of global average sea-level rise exceeded 10 mm/yr, with >40 mm/yr during meltwater pulses [*Fairbanks*, 1989; *Stanford et al.*, 2006; *Deschamps et al.*, 2012]. During the Common Era (CE), global average sea-level rise was slow (0–0.6 mm/yr) until the late 19th century [*Gehrels and Woodworth*, 2012]. The global average rate of sea-level rise from 1880 to 2006 CE was 1.7 ± 0.2 mm/yr with a slight acceleration [*Church et al.*, 2011; estimates for the 20th century range from 1.53 ± 0.19 to 1.73 ± 0.15 mm/yr; *Gregory et al.*, 2012]. The rate of global average sea-level rise measured from 1993 to 2013 by satellite altimetry is 3.2 ± 0.4 mm/yr [*Nerem et al.*, 2010] (CU Sea Level Research Group, 2013, Published online, http://sealevel.colorado.edu/). This rate appears to be globally accelerating [*Church and White*, 2006, 2011; *Jevrejeva et al.*, 2008; *Rignot et al.*, 2011], but the rate of acceleration is poorly constrained.

Sea level is rising globally due to warming oceans (thermal expansion), which contributed ∼0.3–0.6 mm/yr during the 20th century [*Gregory et al.*, 2012], and the melting of land ice. Mountain glaciers contributed ∼0.6–1.1 mm/yr in the 20th century [*Gregory et al.*, 2012]. The contribution of the melting of continental ice sheet during the 20th century is poorly constrained, with the Greenland Ice Sheet (GIS) contribution estimated between −0.3 and +0.3 mm/yr [*Gregory et al.*, 2012]. From 1992 to 2011, the GIS, West Antarctic ice sheet, and East Antarctic ice sheet contributions are estimated at 0.6 ± 0.2 mm/yr [*Shepherd et al.*, 2012].

At the time of IPCC's (International Panel on Climate Change) Fourth Assessment Report [AR4; *IPCC*, 2007], the contribution of mass from the Greenland, West Antarctica, and East Antarctica ice sheets was poorly known. AR4 [*Meehl et al.*, 2007] projected a sea-level rise for 2100 CE of ∼40 ± 20 cm, but their estimates did not include accelerating ice sheet discharge. However, the melting of continental ice sheets does appear to be accelerating, at least transiently, with ice sheets contributing 1.0 ± 0.1 mm/yr to global average sea-level rise from 2005 to 2010 CE [*Shepherd et al.*, 2012].

The IPCC Fifth Assessment Report [AR5; *IPCC*, 2013] attempted a more comprehensive assessment of sea-level rise. Its projections are based primarily on physical ocean and ice sheet models. For the two concentration pathways plausibly representing socioeconomic scenarios without extensive mitigation policy (RCP 6.0 and RCP 8.5), AR5's "likely" GSL rise projections for 2081–2100 extend from 33 cm (the 17th percentile of RCP 6.0) to 82 cm (the 83rd percentile of RCP 8.5) above a 1986–2005 baseline. In large part because of the limitations of physical process models, AR5 does not offer sea-level projections above the 83rd percentile, although for investment and adaptation decisions, risks with a probability of <17% can be highly pertinent.

Other approaches, based on semiempirical models [e.g., *Rahmstorf*, 2007; *Schaeffer et al.*, 2012; *Grinsted et al.*, 2009; *Rahmstorf et al.*, 2012], and/or expert judgment, including the integration of multiple sources of data [e.g., *Katsman et al.*, 2011; *National Research Council* (NRC), 2012], span a wider range and include upper limits considerably higher than those projected by the IPCC. Current semiempirical models, based on the past statistical relationship between the rate of sea-level rise and temperature, project a 90% probability of ∼70–140 cm rise between 2000 and 2100 CE under a business-as-usual scenario [*Schaeffer et al.*, 2012]. Extrapolating a possible acceleration noted in Gravity Recovery and Climate Experiment (GRACE) and satellite altimetry data [*Rignot et al.*, 2011] led the NRC (2012; NRC12) to propose a central estimate of ∼80 cm global average sea-level rise between 2000 and 2100 CE, with low and high scenarios spanning 50–140 cm. In this paper, we use global average sea-level scenarios that follow NRC12's approach, but employ new ice sheet mass loss data [*Shepherd et al.*, 2012]. The extrapolation of ice sheet mass loss is inherently limited by the short observation period (∼20 years), which is a major source of uncertainty in GSL rise scenarios, including ours. We also include AR5's projections of the effect of changes in water storage on land, a factor omitted from NRC12.

Relative sea level is affected by global average sea level (including variations in ocean temperature and ice volume), regional and local subsidence or uplift (including thermal subsidence, sediment loading,

Table 1. Sea-Level Rise Scenarios[a]

	Global					Regional			Local	Totals		
	Thermal Exp. (cm)	Glaciers (cm)	GIS (cm)	AIS (cm)	Water Storage (cm)	Oceanographic (cm)	Static Equilibrium (cm)	GIA (cm)	Coastal Subsidence (cm)	GSL (cm)	Bed-Rock (cm)	Coastal Plain (cm)
2030 central	5	3	3	2	1	6	−2	4	3	14	22	25
2030 low	2	3	1	1	0	2	−1	3	2	9	16	19
2030 high	11	4	4	6	2	8	−2	5	4	22	31	34
2030 higher	11	4	4	6	2	8	−2	5	4	27	38	41
2050 central	10	6	8	2	2	10	−4	7	5	25	40	45
2050 low	4	5	2	1	−1	3	−2	5	4	16	28	33
2050 high	19	7	10	9	4	13	−5	9	6	39	53	59
2050 higher	19	7	10	9	4	13	−5	9	6	49	65	71
2100 central	24	14	27	8	4	20	−14	13	10	77	96	106
2100 low	10	13	4	2	−1	5	−4	9	8	43	66	76
2100 high	46	19	35	33	8	25	−15	17	12	121	140	150
2100 higher	46	19	35	33	8	25	−15	17	12	141	168	180

[a]All values with respect to a 2000 baseline. GIS = Greenland Ice Sheet; AIS = Antarctic Ice Sheet; GIA = glacial isostatic adjustment; GSL = global sea level.

flexural, and glacial isostatic adjustment (GIA) effects), gravitational, rotational, and flexural effects due to changing ice sheets (collectively known as "static equilibrium" effects) [*Kopp et al.*, 2010], and oceano-graphic effects (including dynamic topography and tidal-range change effects) [*Mitrovica and Milne*, 2003; *Milne et al.*, 2009]. In the mid-Atlantic region, the rate of relative sea-level rise was nearly double the rate of global average sea-level rise during the 20th century (Figure 2) due to GIA, sediment compaction (natural and groundwater effects), and oceanographic effects [*Miller et al.*, 2009; *Horton et al.*, 2013].

In this paper, we (1) evaluate relative sea-level rise in New Jersey over the Holocene (last 11.7 kyr) using geological data and in the wider U.S. mid-Atlantic region since 1900 using tide-gauge records; (2) quantify the contributions of global rise and subsidence due to thermal-flexural subsidence, GIA, and compaction effects; (3) provide relative sea-level projections for 2030, 2050, and 2100 CE for the region accounting for GSL rise, regional and local subsidence, and oceanographic effects (Table 1); and (4) illustrate the effects of relative sea-level rise on future storm surges.

2. Methods

2.1 Computing Rates of Holocene Sea-Level Rise Using Geological and Tide-Gauge Data

Our Holocene sea-level database for New Jersey [*Engelhart et al.*, 2009; *Engelhart and Horton*, 2012; *Horton et al.*, 2013] consists of 50 sea-level index points and 10 limiting dates that define continuously rising relative sea level (Figure 2). The New Jersey data were derived from sites with minimal autocom-paction (the process affecting sediments in cores with overburden, which is distinct from the regional process of compaction of the entire coastal plain) because they lie on less compressible sediments (generally sand), although compaction of the underlying strata does occur, albeit at very slow rates (see following text section 3). [*Horton et al.*, 2013]. The database of sea-level index points is complemented by a continuous and detailed reconstruction of CE sea level from two sites in southern New Jersey [*Kemp et al.*, 2013].

To compute the relative sea-level curve (Figures 2a and 2b), we include tide-gauge data from Atlantic City, NJ. We also present trends in tide-gauge data from the mid-Atlantic region (Figure 1) that have been smoothed using the Gaussian process method of *Kopp* [2013] to remove interannual red-noise-like variability. This method uses observations of mean annual sea level from 47 eastern North America tide gauges archived by the Permanent Service for Mean Sea Level (http://www.psmsl.org/), each with a
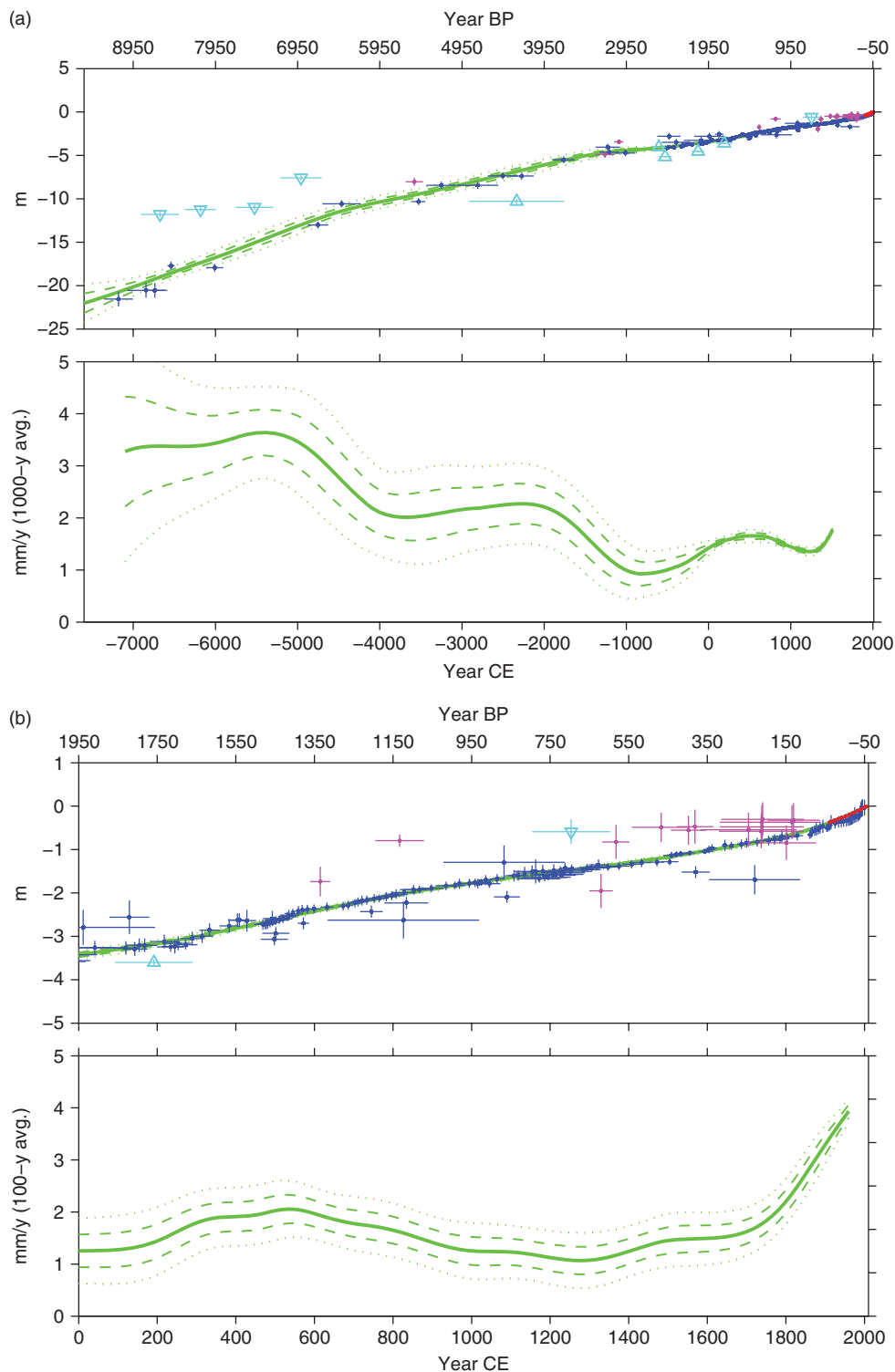
Figure 2. (a) Relative sea-level change over the past 10,000 years in New Jersey using dataset compiled by *Horton et al*. [2013] and *Kemp et al*. [2013] for basal (blue) and intercalated (magenta) dates and smoothed Atlantic City tide-gauge data (red); cyan = limiting dates with upward for marine limiting and downward for freshwater limiting, all with 2σ error bars. Smoothed line (green) along with 1σ (thick dashed line) and 2σ (thin dashed line) errors are shown. Bottom plot shows 1000 year average rates of change, plotted at the central year of each 1000 year interval. (b) Enlargement of the Common Era; smoothed line (red) along with 1σ (thick dashed line) and 2σ (thin dashed line) errors are shown. Bottom plot shows 100 year average rate of change, plotted at the central year of each 1000 year interval. See (a) for description.

record length exceeding 30 years, to model the spatiotemporal field of sea level during the instrumental period.

To analyze the data, we apply a Gaussian process regression methodology similar to that used by *Kopp* [2013] for tide-gauge analysis. Vertical errors on index points in the database were treated as normally distributed. Uncertainty on calibrated ages was transformed to vertical uncertainty using the noisy-input Gaussian process methodology of *McHutchon and Rasmussen* [2011]. We fit the data to a Gaussian process with a prior mean of zero and prior covariance function $k(t_1,t_2)$, where t_1 and t_2 are two different ages. We employ the sum of a Matérn covariance function with amplitude σ_m^2, scale factor τ, and order γ and white noise with amplitude σ_n^2. As *Horton et al*. [2013] did not include errors from their compaction correction, the observation errors are incremented by a fraction of the compaction correction. Specifically, the observation variance σ_x^2 used is equal to the sum of the reported variance σ_r^2 and $(fc)^2$, where f is a hyperparameter and c the compaction correction. We set the hyperparameters σ_m, τ, γ, σ_n, and f by finding their maximum likelihood values. The resulting hyperparameters are $\sigma_m = 22.8$ m, $\tau = 17.9$ kyr, $\gamma = 1.4$, $\sigma_n = 0.0$ mm, and $f = 0.84$.

To compute the probability distribution for the last interval in which the rate of sea-level rise in New Jersey exceeded its 20th century level, we took 10,000 samples from the posterior probability distribution for the rate of sea-level change, taking into account the covariance among time points.

2.2 Constructing Scenarios of Future Relative Sea-Level Rise

Four scenarios of 21st century relative sea-level rise (Table 1) were constructed accounting for the effects of (1) GSL rise due to thermal expansion, (2) GSL rise and regional static-equilibrium "fingerprint" effects due to the melting of glaciers, small ice caps, and ice sheets, (3) glacial isostatic adjustment, (4) local subsidence, and (5) ocean dynamics. We interpolate between the four time points of our estimate (2000, 2030, 2050, and 2100) quadratically. Our projections for GSL rise follow an approach modified from NRC12.

Thermal expansion. Following NRC12, who drew upon *Pardaens et al*. [2011], the "central" scenario is based on the median of Coupled Model Intercomparison Project 3 (CMIP3) GCM estimates for the A1B (medium emissions) scenario. The "low" scenario is based on the 5th percentile of CMIP3 GCM estimates for the B2 (low emissions) scenario. The "high" and "higher" scenarios are based on the 95th percentile of CMIP3 GCM estimates for the A1FI (high emissions) scenarios.

Mountain glaciers and small ice caps. Again following NRC12, rates of glacier ice mass loss are extrapolated from 1960 to 2005 observations assuming constant acceleration (low and central cases) or with an additional contribution from a rapid dynamic response (high and higher scenarios). Based on data from *Mitrovica et al*. [2001], we employ a static equilibrium sea-level fingerprint of 0.85 m local sea level change/1.0 m GSL change for the glaciers and ice cap contribution. The slightly-less-than-1 value reflects the relative proximity of the mid-Atlantic region to major melting glaciers in Alaska, Arctic Canada, and Iceland.

Ice sheet contributions. NRC12 estimated the contribution of ice sheet melt by extrapolating the compilations of ice mass accumulation and loss (mass balance), which extend from 1992 to 2010 for the Greenland and Antarctic ice sheets [*Rignot et al*., 2011]. We update these global estimates using a recent synthesis of ice loss observations in Greenland and Antarctica [*Shepherd et al*., 2012].

We consider three cases of ice sheet melt. In the low case, we assume that Greenland and Antarctic melt continue at the same average rate as observed over the interval for 1992–2011: -142 ± 49 Gt/yr for Greenland and -71 ± 53 Gt/yr for Antarctica. We assume that melt follows the median of these rate estimates, which translate to 0.4 and 0.2 mm equivalent sea level (esl)/yr, respectively. These rates yield 39 and 19 mm of esl rise between 2000 and 2100.

In the central case, we assume that the decadal acceleration observed between 1992–2000 and 2000–2011 continues. This acceleration amounts to esl -16.8 ± 7.9 Gt/yr^2 (median of 0.046 mm/yr^2) and -4.1 ± 8.2 Gt/yr^2 (median of 0.011 mm/yr^2). These rates yield 270 mm for GIS and 80 mm for AIS between 2000 and 2100. The 77 mm of esl rise for AIS is net of 120 mm loss from the West Antarctic Ice Sheet (WAIS) and 40 mm growth of the East Antarctic Ice Sheet (EAIS) a and is within the upper limits of observations by *Little et al*. [2013].

In the high case, we assume that the acceleration observed over the first decade of the 21st century (-22.9 ± 18.8 Gt/yr^2; ~ 0.06 mm/yr^2) in Greenland continues through the century and that Antarctic ice melt accelerates at a similar rate. This yields esl contributions of 350 mm for GIS and 330 mm for AIS over the course of the 21st century. The 330 mm of esl for AIS is outside of the upper limits of 130 mm of observations by *Little et al.* [2013], implying that it requires regional collapse of marine-based sectors of the ice sheet.

Based on observations by *Mitrovica et al.* [2001], we employ a static equilibrium sea-level fingerprint of 0.5 for average Greenland melt. For the Antarctic, based on the analysis by *Mitrovica et al.* [2011], we employ a static equilibrium sea-level fingerprint of 1.15 (calculated for a mixture of West Antarctic melt (1.25) and East Antarctic melt (1.05)).

Water storage. NRC12 did not consider the GSL effect of changes in water storage on land due to ground-water extraction and dam construction. Based on AR5, we employ a GSL contribution of water storage on land of 4 cm (range of -1 to 8 cm) in 2100. We assume that these levels are approached linearly over the course of the century.

Glacial isostatic adjustment. We employ a GIA rate estimate of 1.3 ± 0.4 mm/yr (2σ) based on observations by *Kopp* [2013] and *Engelhart and Horton* [2012].

Ocean dynamics. Based on *Yin et al.*'s [2009] analysis of the models documented in the IPCC Fourth Assessment Report, we employ an ocean dynamic contribution to sea-level rise in 2100 of 20 cm, with a 95% confidence range of 5–25 cm. We assume that these levels are approached linearly over the course of the century.

Coastal subsidence. Based on the analysis by *Kopp* [2013] of the tide-gauge records at Atlantic City and Sandy Hook, we employ a subsidence rate of 1.0 ± 0.2 mm/yr for coastal plain localities.

Correlation among terms. In the low and high scenarios, we combine terms together by assuming that differences from the central scenario for the land ice terms add linearly (i.e., uncertainties in land ice behavior are strongly correlated). Differences from the central scenario for total land ice and for other terms are added quadratically (i.e., uncertainties are assumed to be independent). In the higher scenario, all differences are added linearly (i.e., uncertainties are assumed to be strongly correlated). Some of these correlations (e.g., between the dynamic sea-level rise and GIS melt, which might promote Atlantic Meridional Overturning Circulation (AMOC) slowdown) have plausible physical interpretations; others should be viewed simply as bracketing an extreme state of the world.

Physically plausible upper bound. To estimate a physically plausible upper bound, we start with *Pfeffer et al.* [2008]'s estimate of 2.0 m sea-level rise over the 21st century. *Pfeffer et al.* [2008] assumed a 30 cm contribution for thermal expansion, whereas *Sriver et al.* [2012] estimate a physically plausible upper bound to the thermal expansion contribution of 55 cm. *Pfeffer et al.* [2008] estimated a maximum Antarctic contribution of 62 cm, whereas *Bamber and Aspinall* [2013] estimate a 95th percentile rate of West Antarctic and East Antarctic melt in 2100 equivalent to 11.8 and 10.2 mm/yr GSL rise. Assuming this contribution of ~ 22 mm/yr is reached quadratically over the remainder of the century yields an Antarctic contribution of ~ 94 cm. Factoring in the water storage contribution yields a GSL estimate of 2.7 m. If the oceanographic contribution to sea-level rise in the mid-Atlantic region is ~ 35 cm (the maximum of the models evaluated by *Yin et al.* [2009]), static equilibrium effects are taken into account and GIA and coastal subsidence are as in the higher scenarios; these correspond to 3.0 m at the Battery and 3.1 m at Atlantic City.

3. Sea-Level History From Holocene Geological Records

Evaluation of Holocene sea-level changes allows us to quantify subsidence processes that are important contributions to relative sea-level rise today (e.g., $\sim 50\%$ of the relative rise in tide gauges at Atlantic City and Sandy Hook, NJ, today is due to subsidence; Figure 3). The mid-Atlantic region is a passive continental margin with thick (>16 km) Jurassic to Holocene deposits (~ 180–0 Ma) in the Baltimore Canyon Trough basin (Figure 1), where subsidence was controlled by simple thermal subsidence, loading, and compaction following rifting [~ 220–198 Ma; *Watts and Steckler*, 1979]. The onshore coastal plain consists of Cretaceous to Holocene unconsolidated sands, silts, clays, and gravels. Coastal plain subsidence has been dominated by thermoflexural (the combination of thermal subsidence and sediment
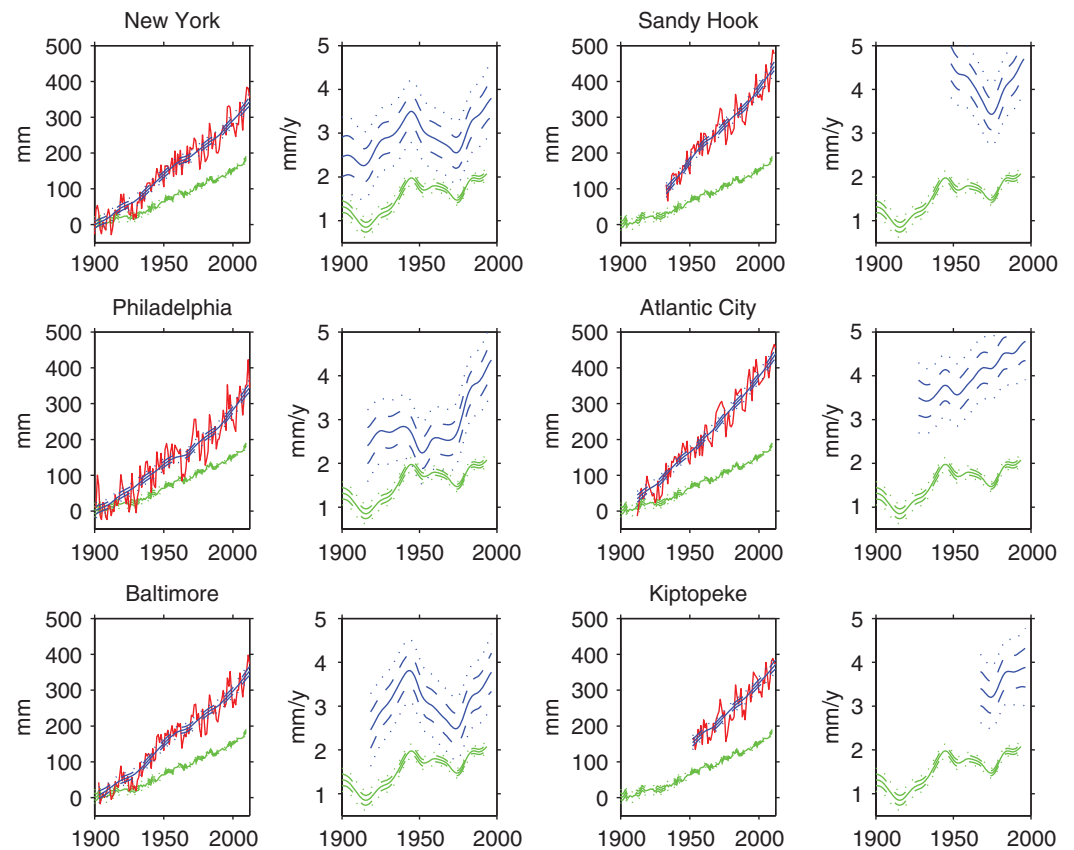
Figure 3. Examples of tide-gauge analyses for sites along the Fall Line (left columns) and in the coastal plain (right columns) [*Kopp*, 2013]. In the first panel for each site are the data (red), the modeled underlying sea level with red-noise-type variability removed (blue, see text for analysis procedure), and the average global sea level (GSL) derived from tide-gauge records [green, *Church and White*, 2011]. In the second panel are the 31 year average rates of change with 1σ (thick dashed lined) and 2σ (thin dashed line) uncertainties.

loading offshore, producing flexural subsidence onshore) and compaction effects since the Cretaceous [*Kominz et al*., 1998]. The Fall Line separates compressible coastal plain sediments from incompressible bedrock of the Piedmont Province that includes Paleozoic metasediments and Triassic to Jurassic rift basin rocks (Figure 1).

Coastal plain sediments record a Holocene relative sea-level rise in the mid-Atlantic region [e.g., *Miller et al*., 2009; *Psuty*, 1986]. Here, we compute the probability distribution of Holocene relative sea-level rise in New Jersey after assimilating the database and continuous sea-level reconstructions to estimate rates of change and attendant errors (see section 2). Our analysis of the Holocene sea-level database of New Jersey (Figure 2a) shows that after the major phase of deglaciation (circa 20–9 ka), the rate of sea-level rise decreased from 3.5 ± 1.0 mm/yr (2σ) at 7.5–6.5 ka to 2.2 ± 0.8 mm/yr at 5.5–4.5 ka; it further decreased to a minimum of 0.9 ± 0.4 mm/yr at 3.3–2.3 ka. In the CE (Figure 2b), the rate increased from this minimum, with sea-level rising at 1.6 ± 0.1 mm/yr from 2.2 to 1.2 ka (800 CE) and at 1.4 ± 0.1 mm/yr from 800 to 1800 CE.

The combination of geological proxies and tide-gauge data shows that relative sea-level rise throughout the mid-Atlantic region has been more rapid since the Industrial Revolution, rising at 2.7 ± 0.4 mm/yr in the 19th century and at 3.8 ± 0.2 mm/yr in the 20th century [*Kopp*, 2013; see below]. There is a 99% probability that the rate of sea-level rise in New Jersey in the 20th century was faster than in any century in the last 3.8 kyr, a 95% probability that it was faster than in any century in the last 4.3 kyr, and a 67% probability that it was faster than in any century since over the last 6.6 kyr.

This compaction and tidally corrected New Jersey relative sea-level record (Figure 2) is generally similar to relative sea-level records from this region (e.g., Virginia, Chesapeake Bay, Delaware, New York, and southern New England [*Engelhart and Horton*, 2012]). However, compaction and tidal corrections are needed for these Holocene datasets before detailed comparisons are made.

The northern part of the mid-Atlantic region was potentially affected by direct isostatic loading effects (i.e., within the effects of flexural loading ~100–300 km from the load) of the ice sheet that extended to 40.5°N [*Stanford et al.*, 2002]. However, studies of marsh sediments from the northern New Jersey coast (e.g., Cheesequake, NJ [*Psuty*, 1986]; Figure 1) show patterns similar to the rest of New Jersey. This location is less than 30 km from the Laurentide terminal moraine, and suggests that contrary to prior suggestions [*Dillon and Oldale*, 1978], the proximal effects of the Laurentide ice sheet are negligible from New Jersey to the south, at least during the Holocene [see also *Goff et al.*, 2013]. GIA subsidence dominates the nonglobal component of Holocene relative sea-level rise in the mid-Atlantic region. *Peltier* [2004] estimated that GIA subsidence is currently ~1.3 mm/yr throughout this region. The *Engelhart et al.* [2009] late Holocene sea-level database exhibits GIA subsidence rates between 1.2 and 1.7 mm/yr.

4. Sea-Level History From Tide Gauges

We evaluate trends in tide-gauge data in the mid-Atlantic region in a geological context. *Kopp* [2013] estimated the spatiotemporal field of sea level along the U.S. east coast (see section 2). His method accommodates data gaps, allows decomposition of signals into local, regional, and global components, and into linear trends, a smooth, nonlinear long-term trend, and red noise-type short-term variability (Figure 3). It also accounts for differences in record length of tide gauges and allows sea level at all sites to be referenced to a common base year (1900 CE). The pattern of GIA can be clearly seen in the analysis [*Kopp*, 2013], which supports a GIA-associated sea-level rise of about 1.3 ± 0.4 (2σ) mm/yr for the mid-Atlantic region from New York to Maryland.

Relative sea-level rise at all mid-Atlantic locations exceeds the global rise (Figures 1 and 3). Tide gauges on bedrock sites located on or near the Fall Line (New York City, Philadelphia, Baltimore, and Washington, D.C.; Figures 1 and 3) show trends of ~3 mm/yr (i.e., ~1.3 mm/yr above the global trend) [*Church and White*, 2006, 2011]. The consistency among these sites supports the interpretation that, during the Holocene, regional subsidence at bedrock locations is almost entirely due to GIA effects (vs. near-field effects) [*Dillon and Oldale*, 1978].

Coastal plain locations experience relative sea-level rise higher than bedrock locations. Coastal plain locations show rates of ~3.3–4.3 mm/yr, about 0.3–1.3 mm/yr above the rates observed at bedrock sites, and ~1.6–2.6 mm/yr above global average sea-level rise (Figures 1 and 3). In New Jersey, relative sea-level rise at coastal plain locations is greater than at bedrock sites by 0.6–1.0 mm/yr (Figure 1). Differences from bedrock sites are generally less in the Delaware, Maryland, and Virginia coastal plains (0.3–0.7 mm/yr), with the exception of Sewell's Point, Virginia, which shows a 1.3 mm/yr difference (Figure 1).

The coastal plain is affected by subsidence due to long-term (10^7–10^6 yr) thermoflexural effects and compaction due to sediment loading and groundwater withdrawal. Today, thermoflexural subsidence in this region is less than 10 m/Myr (0.01 mm/yr) and subsidence due to deep (pre-Holocene) compaction is less [*Kominz et al.*, 2008; *Hayden et al.*, 2008]. *Yu et al.* [2012] similarly quantified low (<0.15 mm/yr) thermoflexural subsidence (including deep compaction) in the Mississippi delta region.

The 0.3–1.3 mm/yr additional sea-level rise in the coastal plain (Figure 1) cannot entirely be attributed to natural compaction of Holocene strata. The Holocene sections at Sandy Hook, Atlantic City, and Cape May are ~51, 41, and 23 m thick, respectively [*Minard*, 1969; *Miller et al.*, 2009]. Decompaction of the three Holocene sections following *Kominz et al.* [2011] would yield subsidence of 0.9, 0.85, and 1.8 m, respectively, although the errors on decompaction are large (±20% in the upper 100 m). Age control is poor, but deposition of these sections appears to have begun during the slowdown of sea-level rise over the past 3–5 kyr. This yields maximum rates of subsidence (assuming the sections are younger than 3–5 ka, i.e., the time when shorelines stabilized) due to Holocene compaction of 0.3, 0.3, and 0.6 mm/yr, respectively. Minimum rates of subsidence due to Holocene compaction are 0.09, 0.085, and 0.18, assuming basal sediments are ~10 ka.
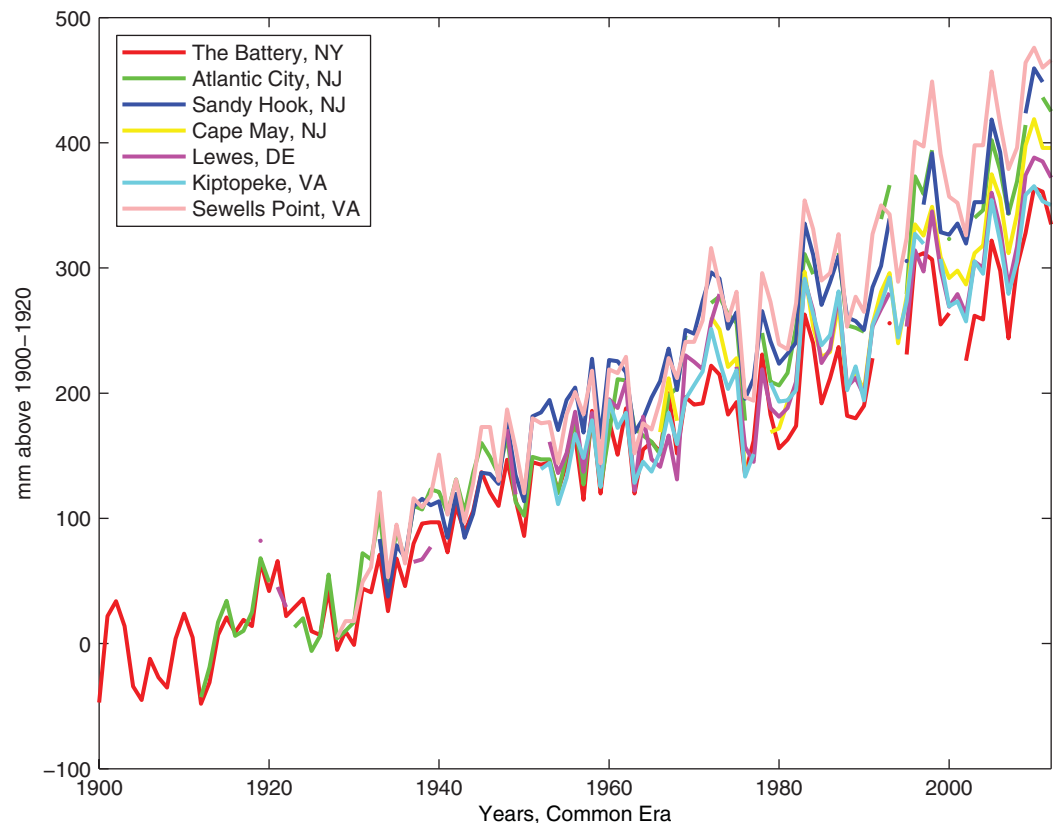
Figure 4. Comparison of tide gauges along the coast with the Battery. The tide-gauge records are referenced to a synthetic 1900–1920 datum, inferred based on the Gaussian process sea-level model of *Kopp* [2013].

Comparison of tide gauges shows coherent interannual variability at the coastal sites (Sandy Hook, Atlantic City; Cape May, NJ; Lewes, DE; Sewells Point, VA) and the Battery, NY (Figure 4). The coherent interannual variability of the ocean coastline tide gauges (Figure 4) is likely due to oceanographic effects such as those associated with changes in the Gulf Stream-North Atlantic Current [*Ezer et al.*, 2013] and/or Atlantic Meridional Overturning Circulation [*Yin et al.*, 2009]. *Kopp* [2013] noted correlations between sea level at New York and changes in Atlantic Multidecadal Oscillation (AMO) index (positively correlated with the AMO index leading by 7 years), the North Atlantic Oscillation (NAO) index (anticorrelated with the NAO index leading by 2 years), and the migration of the Gulf Stream North Wall (anticorrelated), all of which would dynamically alter sea level. However, the higher rates at the coastal plain sites on the decadal to centennial scales (Figures 1, 3, and 4) compared to bedrock sites (represented in Figure 4 by the Battery, NY) cannot be attributed to oceanographic effects because they are not found throughout the region that should be affected by changes in ocean dynamics. For example, the Battery record is coherent interannually (red line, Figure 4) with coastal plain sites, but diverges from coastal plain sites including Sandy Hook (dark blue line, Figure 4) in the mid-20th century despite their close proximity. The notable exception among coastal plain sites is Kiptopeke, VA, whose long-term trend tracks closer to the Battery, NY, than other coastline locations (Figure 4).

We suggest that groundwater withdrawal plays an important role in the relative sea-level rise in the mid-Atlantic region, similar to other regions in the late 20th century [*Galloway and Sneed*, 2013]. Groundwater withdrawal rates are high (>10 million gallons per day) in Atlantic County, NJ, from the 800 foot sand aquifer. An additional 10 million gallons per day are withdrawn from the 800 foot sand aquifer in Ocean and Cape May Counties [*McAuley et al.*, 2001]. Groundwater mining affects subsidence in this area [*Leahy and Martin*, 1993]. Subsidence of 1.7 cm was measured in Atlantic City from 1981 to 1995 CE [*Sun et al.*, 1999]. Subsidence from 1980 to 2007 CE due to groundwater withdrawal was 2.2 cm [*O. Zapecza*, USGS written communication, 2013], with a linear fit of 0.79 ± 0.013 mm/yr. Examination of the maps of cones

of depression from groundwater withdrawals shows extensive influence throughout New Jersey coastal locations [*DePaul et al*., 2003]. *Pope and Burbey* [2004] ascribed subsidence rates of 1.4–3.7 mm/yr to groundwater withdrawal in Virginia, and this excess subsidence can close the relative sea-level budget in the Virginia "hotspot" [*Cronin*, 2012]. Further study of groundwater withdrawal and its relationship to subsidence is needed, especially where extraction rates are lower, such as at Lewes, DE [~1.5 million gallons per day; *Andres et al*., 2003] and Sandy Hook, NJ [*DePaul et al*., 2003]. Nevertheless, the divergence of coastal sites (except rural Kiptopeke) from bedrock records (e.g., the Battery) (Figure 4) appears to occur in the mid-20th century and thus appears to be due to groundwater extraction. We note that groundwater extraction rates in the Atlantic coastal plain were low prior to 1900 CE, accelerated in the 20th century, and stabilized from 1980 to the present [*DePaul et al*., 2007].

5. Future Relative Sea-Level Projections

Employing different sets of assumptions about the continuation of observed ice-loss accelerations and the correlation between different contributors to sea-level rise, we estimate a GSL rise from a 2000 CE baseline of 14 cm (central scenario; low-to-higher scenario range of 9–27 cm) by 2030, 25 cm (range 16–49 cm) by 2050, and 77 (range 43–141 cm) by 2100 (Table 1; see section 2 for details). Our scenarios are similar to those of NRC12 (2100 central estimate of 80 cm; range 51–140 cm). Accounting for the difference in time period, our central scenario is similar to the AR5 central estimate for RCP 8.5 (63 cm above 1986–2005 in 2081–2100), and our low scenario is similar to the 17th percentile of the AR5 estimate for RCP 6.0 (33 cm above 1986–2005 in 2081–2100). Our high and higher scenarios are intended to span a greater range of probability space than AR5's 83rd percentile estimate for RCP 8.5 (97 cm), thus providing more useful guidance for risk management. The 2100 intermediate-high (120 cm) and intermediate-low (50 cm) scenarios recorded by *Parris et al*. [2012] are in general agreement with our scenarios. The highest scenario (200 cm) estimates of *Parris et al*. [2012] are significantly higher than our higher scenario, as it is based on *Pfeffer et al*. [2008]'s estimate of the maximum physical plausible ice loss. An updated consideration, however, suggests that a physical upper bound to 21st century GSL rise might be closer to 2.7 m (see section 2). We do not include such a worst-case scenario in Table 1.

We add the regional effects of subsidence, oceanographic changes, and ice/ocean mass redistribution (static equilibrium sea level) to obtain projections of relative sea-level rise for the mid-Atlantic region (see section 2). Our scenario-based projections are that relative sea level will rise at bedrock locations like the Battery by 22 cm by 2030 (range 16–38 cm), 40 cm by 2050 (range 28–65 cm), and 96 cm by 2100 (range 64–168 cm). Our scenarios compare with the New York City Panel on Climate Change (NPCC2; Climate risk information 2013: Observations, climate change projections, and maps, 2013, http://www.nyc.gov/html/planyc2030/downloads/pdf/npcc_climate_risk_information_2013_report.pdf)'s estimates of a 10th/25th/75th/90th percentile for sea-level rise at the Battery in the 2050s of 18/28/61/78 cm, relative to a 2000–2004 baseline. The broader range in NPCC2 arises primarily from the use of *Bamber and Aspinall* [2013]'s fat-tailed expert elicitation study to estimate probabilistically ice sheet mass loss.

Sea-level rise on the coastal plain will be higher. Assuming groundwater extraction rates similar to those in late 20th century and attendant total compaction subsidence of $\sim 1.0 \pm 0.2$ mm/yr, coastal plain sites impacted by groundwater and natural compaction will experience a rise of 25 cm by 2030 (range 19–41), 45 cm by 2050 (range 33–71 cm), and 106 cm by 2100 (range 76–180 cm). Coastal locations with lower groundwater extraction rates and coastal plain locations closer to the Fall Line (e.g., with an excess of subsidence of 0.3–0.6 mm/yr; Figure 1) will experience sea-level rise intermediate between these two estimates.

Our estimates quantify the regional and local contributions to sea-level rise in the past (Figure 2), present, and future (Figure 5). From circa 2 ka to the 20th century, subsidence was the dominant component. In the 20th century, global and subsidence processes have had similar influence. Although the dominant component in the 21st century will be changes in global mean sea level (~90% for bedrock sites and ~80% at coastal plain sites), the ~10–30 cm rise due to subsidence at bedrock and coastal plain sites (Figure 5), respectively, must be accounted for in planning.
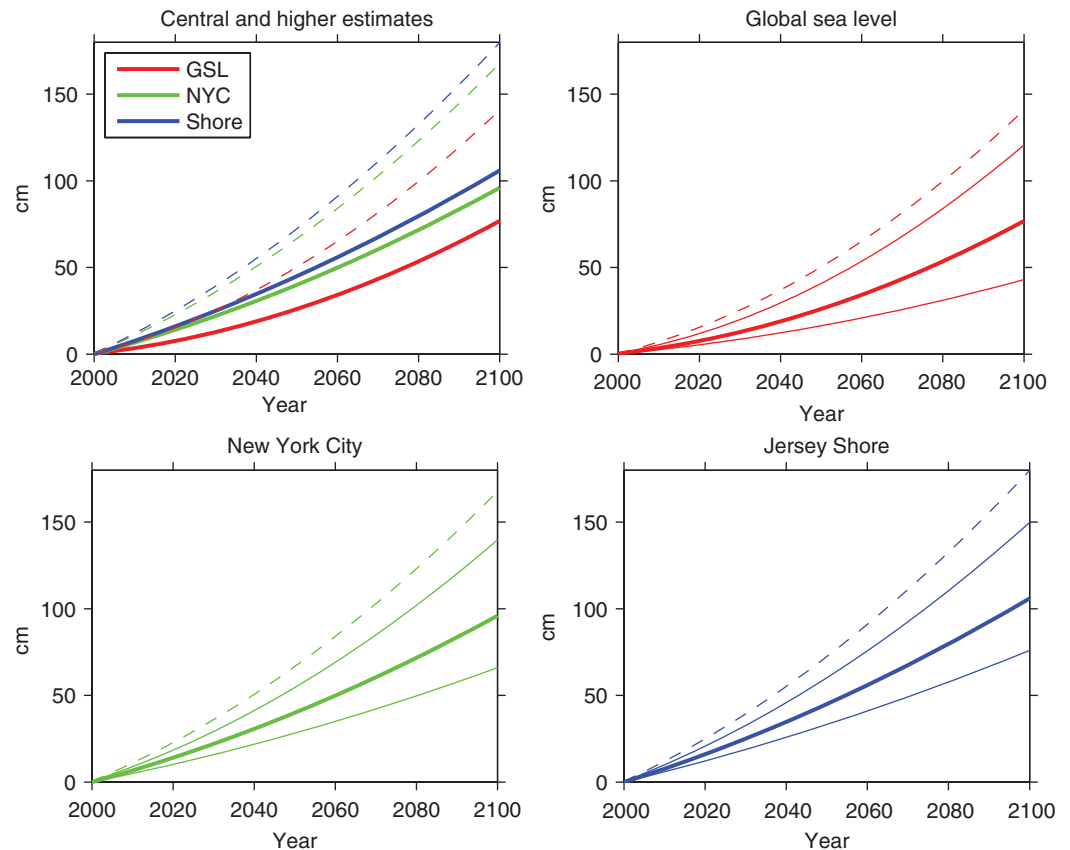
Figure 5. Projections of global sea-level (GSL) rise, relative sea-level rise at New York City, and relative sea-level rise on the Jersey shore. In the upper left plot, central (heavy solid) and higher (dashed) scenarios are shown for GSL (red), New York City (green), and the Jersey shore (blue). In the other three plots, low (solid) and high (upper solid) scenarios are also shown.

6. Implications of Sea-Level Rise to Future Storm Tides

National Oceanic and Atmospheric Administration (NOAA) compiled extreme storm tide statistics for all of its tide-gauge stations in its network and recurrence intervals for various storm tides [e.g., "100 year storms"; *Zervas*, 2005] and previous work illustrated the relationship between sea-level rise and storm at the Battery [*Psuty*, 1986; *Horton et al*., 2010, 2011]. We illustrate the effects of sea-level rise on flooding by storm tides using our central scenario of 40 and 96 cm sea-level rise at the Battery and 45 and 106 cm at Atlantic City (Figure 6) in 2050 and 2100, respectively. We also illustrate the higher end scenarios of 168 and 180 cm at the Battery and Atlantic City, respectively. These figures illustrate that a ~40 cm rise, anticipated by ~2050 CE in the central scenario, would result in a moderate storm (e.g., the "10 year" storm of 25 October 1980 CE) reaching the same flood level of a 100 year storm today. By 2100 CE in the central scenario, even a modest nor'easter such as the one that occurred immediately after Superstorm Sandy (8 November 2012) will exceed the current 100 year storm, and it would also exceed all historic storms at Atlantic City. *Tebaldi et al*. [2012] similarly noted that by 2100 the 10 year storm would have the flooding effect of the modern 100 year storm at many other locations along the conterminous United States. By 2100 in the higher scenario, a 10 year storm event will cause flooding at the Battery comparable to Superstorm Sandy.

Planners should account for rising sea levels. The appropriate scenario to use depends on the downside risk associated with under-preparation. For decisions where flooding has relatively low impact, our central regional estimates of 22–25, 40–45, and 96–106 cm rise by 2030, 2050, and 2100, respectively, provide reasonable targets. These projections correspond to GSL estimates of 14, 25, and 77 cm. For decisions where the consequences of flooding are high, prudent planning requires consideration
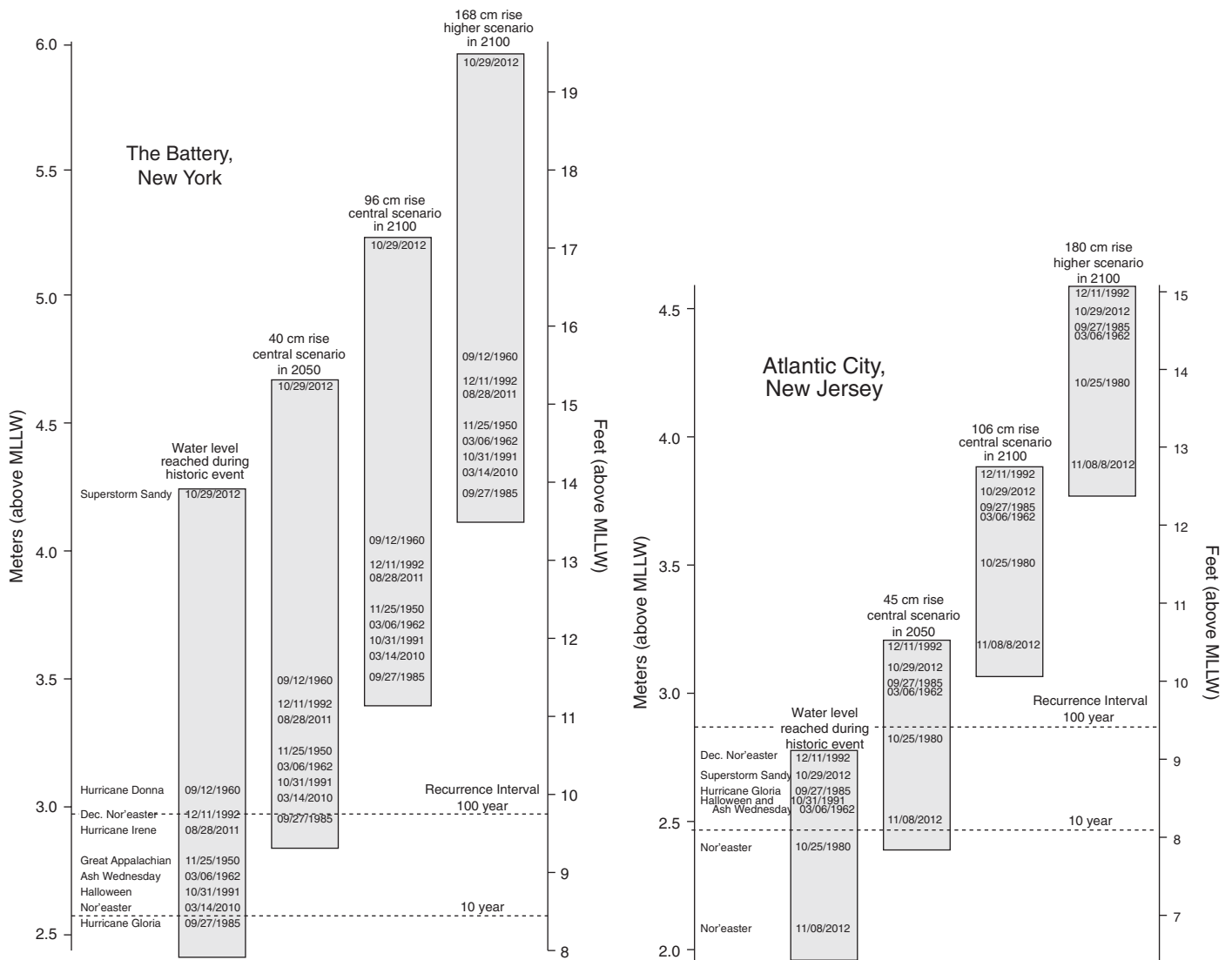
Figure 6. (a) Effects of sea-level rise on storm surge for the Battery assuming relative rises of 40 cm (2050 Common Era [CE]) and 96 cm (2100 CE) (our central scenario) for the first three columns and 168 cm (higher scenario) for 2100 CE for the fourth column. The Advisory Base Flood Elevation for this location is 4.6 m (15 ft mean lower low water, MLLW; 12 ft NAVD88; http://www.region2coastal.com/sandy/table). Adapted after *Psuty* [1986]. (b) Effects of sea-level rise on storm surge for Atlantic City assuming relative rises of 45 cm (2050 CE) and 106 cm (2100 CE) (our central scenario) for the first three columns and 180 cm (higher scenario) for 2100 CE for the fourth column. The Advisory Base Flood Elevation for this location is 5.1 m (16.6 ft MLLW; 14 ft NAVD88; http://www.region2coastal.com/sandy/table). Adapted after *Psuty* [1986].

of high-end projections of 38–41 cm (2030 CE), 65–71 cm (2050 CE), and 168–180 cm (2100 CE). These high-end projections correspond with GSL estimates of 27, 49, and 141 cm.

For decisions that are long-lived and extremely inflexible, and for which flooding would have truly catastrophic consequences, it may be appropriate to consider even higher scenarios, such as a physically plausible but highly unlikely upper limit of ∼2.7 m globally by 2100 [*Pfeffer et al.*, 2008; *Sriver et al.*, 2012; *Bamber and Aspinall*, 2013], which would correspond to ∼3.0 m at the Battery and ∼3.1 m on the coastal plain. In general, however, it would be wiser and more cost-effective to design flexibly and allow for learning as the century proceeds.

Although GSL rise will dominate the relative rise during the 21st century, the difference between global and local sea-level estimates emphasizes the importance of incorporating regional GIA, oceanographic effects, static equilibrium effects, and local compaction into sea-level projections used for multidecadal planning.

In the United States, the recently issued Advisory Basal Flood Elevations (ABFEs) (Federal Emergency Management Agency, Coastal analysis and mapping, 2013, Published online, http://www.region2coastal.com/sandy/abfe) provide an example of the need to incorporate sea-level rise into long-term planning. NOAA's storm recurrence intervals have been incorporated into the ABFEs, but the ABFEs do not include the effects of future sea-level rise. They are accordingly relevant to insuring against current risks but do not provide appropriate guidance for long-term planning. Flooding estimates must take into account future sea-level rise. Additional work is needed to integrate site-specific sea-level rise projections with storm tide statistics to guide planning decisions and investments that may have time frames of 20 years, 40 years, or longer. Future studies are also needed to refine site-specific estimates through the better estimation of local GIA effects within this region and the modeling of the effects of groundwater withdrawal on localized coastal plain subsidence.

References

Andres, A. S., C. A. Duffy, and E. M. Costas (2003), Wellhead protection area delineations for the Lewes-Rehoboth Beach area, *Rept. Invest. No. 65*, pp. 1–23, Delaware Geol. Surv., Newark, N. J.

Bamber, J. L., and W. P. Aspinall (2013), An expert judgment assessment of future sea level rise from the ice sheets, *Nat. Clim. Change*, *3*, 424–427.

Benson, R. (1984), Structure contour map of pre-Mesozoic basement, landward margin of Baltimore Canyon Trough, *Miscellaneous Map Series 2*, Delaware Geol. Surv., Newark, N. J.

Boon, J. D. (2012), Evidence of sea level acceleration at U.S. and Canadian tide stations, Atlantic Coast, North America, *J. Coastal Res.*, *28*, 1437–1445, doi:10.2112/JCOASTRES-D-12-00102.1.

Church, J. A., and N. J. White (2006), A 20th century acceleration in global sea-level rise, *Geophys. Res. Lett.*, *33*, L01602, doi:10.1029/2005GL024826.

Church, J. A., and N. J. White (2011), Sea-level rise from the late 19th to the early 21st century, *Surv. Geophys.*, *32*, 585–602, doi:10.1007/s10712-011-9119-1.

Church, J. A., N. J. White, L. F. Konikow, C. M. Domingues, G. J. Cogley, E. Rignot, J. M. Gregory, M. R. van den Broeke, A. J. Monaghan, and I. Velicogna (2011), Revisiting the Earth's sea-level and energy budgets from 1961 to 2008, *Geophys. Res. Lett.*, *38*, L18601, doi:10.1029/2011GL048794.

Cronin, T. M. (2012), Rapid sea-level rise, *Quat. Sci. Rev.*, *56*, 11–30, doi:10.1016/j.quascirev.2012.08.021.

DePaul, V. T., R. Rosman, and P. J. Lacombe (2003), Water-level conditions in selected confined aquifers of the New Jersey and Delaware Coastal Plain, *USGS Sci. Invest. Rep.* 2008-5145.

DePaul, V. T., D. E. Rice, and O. S. Zapecza (2007), Water-level changes in aquifers of the Atlantic Coastal Plain, predevelopment to 2000, *U. S. Geol. Surv. Sci. Invest. Rep.* 2007-5247, 1–88.

Deschamps, P., N. Durand, E. Bard, B. Hamelin, G. Camoin, A. L. Thomas, G. M. Henderson, J. Okuno, and Y. Yokoyama (2012), Ice-sheet collapse and sea-level rise at the Bølling warming 14,600 years ago, *Nature*, *483*, 559–564, doi:10.1038/nature10902.

Dillon, W. P., and R. N. Oldale (1978), Late Quaternary sea-level curve: Reinterpretation based on glaciotectonic influence, *Geology*, *6*, 56–60, doi:10.1130/0091-7613(1978)6<56:LQSCRB>2.0.CO.

Engelhart, S. E., and B. P. Horton (2012), Holocene sea level database for the Atlantic coast of the United States, *Quat. Sci. Rev.*, *54*, 12–25, doi:10.1016/j.quascirev.2011.09.013.

Engelhart, S. E., B. P. Horton, B. C. Douglas, W. R. Peltier, and T. E. Törnqvist (2009), Spatial variability of late Holocene and 20th century sea-level rise along the Atlantic coast of the United States, *Geology*, *37*, 1115–1118, doi:10.5670/oceanog.2011.28#sthash.BSzTqRqC.dpuf.

Ezer, T., and W. B. Corlett (2012), Is sea level rise accelerating in the Chesapeake Bay? A demonstration of a novel approach for analyzing sea level data, *Geophys. Res. Lett.*, *39*, L19605, doi:10.1029/2012GL053435.

Ezer, T., L. P. Atkinson, W. B. Corlett, and J. L. Blanco (2013), Gulf Stream's induced sea level rise and variability along the U.S. mid-Atlantic coast, *J. Geophys. Res. Oceans*, *118*, 1–13, doi:10.1002/jgrc.20091.

Fairbanks, R. G. (1989), A 17,000 year glacio-eustatic sea level record: Influence of glacial melting rates on the Younger Dryas event and deep ocean circulation, *Nature*, *342*, 637–642, doi:10.1038/342637a0.

Galloway, D. L., and M. Sneed (2013), Analysis and simulation of regional subsidence accompanying groundwater abstraction and compaction of susceptible aquifer systems in the USA, *Bol. Soc. Geol. Mex.*, *65*, 123–134.

Gehrels, W. R., and P. L. Woodworth (2012), When did modern rates of sea-level rise start?, *Global Planet. Change*, *100*, 263–277, doi:10.1016/j.gloplacha.2012.10.020.

Goff, J. A., J. A. Austin Jr., and C. S. Fulthorpe (2013), Reinterpretation of the "Franklin Shore" in the mid-Atlantic bight as a paleo-shelf edge, *Cont. Shelf Res.*, *60*, 64–69, doi:10.1016/j.csr.2013.04.002.

Gregory, J. M., et al. (2012), Twentieth-century global-mean sea-level rise: Is the whole greater than the sum of the parts?, *J. Clim.*, *26*, 4476–4499, doi:10.1175/JCLI-D-12-00319.1.

Grinsted, A., J. C. Moore, and S. Jevrejeva (2009), Reconstructing sea level from paleo and projected temperatures 200 to 2100 AD, *Clim. Dyn.*, *34*, 461–472, doi:10.1007/s00382-008-0507-2.

Hayden, T., M. Kominz, D. S. Powars, L. E. Edwards, K. G. Miller, J. V. Browning, and A. A. Kulpecz (2008), Impact effects and regional tectonic insights: Backstripping the Chesapeake Bay impact structure, *Geology*, *36*, 327–330, doi:10.1130/G24408A.1.

Horton, B. P., S. E. Engelhart, D. F. Hill, A. C. Kemp, D. Nikitina, K. G. Miller, and W. R. Peltier (2013), Influence of tidal-range change and sediment compaction on Holocene relative sea-level change in New Jersey, USA, *J. Quat. Sci.*, *28*, 403–411, doi:10.1002/jqs.2634.

Horton, R. M., V. Gornitz, and M. Bowman (2010), Climate observations and projections, in *Climate Change Adaptation in New York City: Building a Risk Management Response*, edited by C. Rosenzweig and W. Solecki, 41–62, Annals of the New York Academy of Sciences, New York 1185.

Horton, R. M., V. Gornitz, D. A. Bader, A. C. Ruane, R. Goldberg, and C. Rosenzweig (2011), Climate hazard assessment for stakeholder adaptation planning in New York City, *J. Appl. Meteorol. Climatol.*, *50*, 2247–2266, doi:10.1175/2011JAMC2521.1.

Intergovernmental Panel on Climate Change (IPCC) (2007), *Climate Change 2007: The Physical Science Basis*, edited by S. Solomon et al., 996 pp., Cambridge Univ. Press, Cambridge, U. K.

Intergovernmental Panel on Climate Change (IPCC) (2013), *Climate Change 2013: The Physical Science Basis*, edited by T. Stocker et al., 2216 pp., Cambridge Univ. Press, Cambridge, U. K.

Jevrejeva, S., J. S. Moore, A. Grinsted, and P. L. Woodworth (2008), Recent global sea level acceleration started over 200 years ago?, *Geophys. Res. Lett.*, *35*, L08715, doi:10.1029/2008GL033611.

Katsman, C. A., et al. (2011), Exploring high-end scenarios for local sea level rise to develop flood protection strategies for a low-lying delta — The Netherlands as an example, *Clim. Change*, *109*, 617–645, doi:10.1007/s10584-011-0037-5.

Kemp, A. C., and B. P. Horton (2013), Contribution of relative sea-level rise to historical hurricane flooding in New York City, *J. Quat. Sci.*, *28*, 537–541, doi:10.1002/jqs.2653.

Kemp, A. C., B. P. Horton, S. J. Culver, D. R. Corbett, O. van de Plassche, W. R. Gehrels, B. C. Douglas, and A. C. Parnell (2009), Timing and magnitude of recent accelerated sea-level rise (North Carolina, United States), *Geology*, *37*, 1035–1038, doi:10.1130/G30352A.1.

Kemp, A. C., B. P. Horton, J. P. Donnelly, M. E. Mann, M. Vermeer, and S. Rahmstorf (2011), Climate related sea-level variations over the past two millennia, *Proc. Natl. Acad. Sci. U. S. A.*, *108*, 11,017–11,022, doi:10.1073/pnas.1015619108.

Kemp, A. C., B. P. Horton, C. H. Vane, C. E. Bernhardt, D. R. Corbett, S. E. Engelhart, S. C. Anisfeld, A. C. Parnell, and N. Cahill (2013), Sea-level change during the last 2500 years in New Jersey, USA, *Quat. Sci. Rev.*, *81*, 90–104.

Kominz, M. A., K. G. Miller, and J. V. Browning (1998), Long-term and short-term global Cenozoic sea-level estimates, *Geology*, *26*, 311–314, doi:10.1130/0091-7613(1998)026<0311:LTASTG>2.3.CO;2.

Kominz, M. A., J. V. Browning, K. G. Miller, P. J. Sugarman, S. Mizintseva, and C. R. Scotese (2008), Late Cretaceous to Miocene sea-level estimates from the New Jersey and Delaware coastal plain coreholes: An error analysis, *Basin Res.*, *20*, 211–226, doi:10.1111/j.1365-2117.2008.00354.x.

Kominz, M. A., K. Patterson, and D. Odette (2011), Lithology dependence of porosity in slope and deep marine sediments, *J. Sediment. Res.*, *81*, 730–742, doi:10.2110/jsr.2011.60.

Kopp, R. E., J. X. Mitrovica, S. M. Griffies, J. Yin, C. C. Hay, and R. J. Stouffer (2010), The impact of Greenland melt on regional sea level: a partially coupled analysis of dynamic and static equilibrium effects in idealized water-hosing experiments. *Clim. Change.*, *103*, 619–625, doi:10.1007/s10585-010-9935-1.

Kopp, R. E. (2013), Does the mid-Atlantic United States sea-level acceleration hot spot reflect ocean dynamic variability?, *Geophys. Res. Lett.*, *40*, 3981–3985, doi:10.1002/grl.50781.

Leahy, P. P., and M. Martin (1993), Geohydrology and simulation of ground-water flow in the Northern Atlantic Coastal Plain aquifer system, *USGS Prof. Pap. 1404-K*.

Little, C. M., M. Oppenheimer, and N. M. Urban (2013), Upper bounds on twenty-first-century Antarctic ice loss assessed using a probabilistic framework, *Nat. Clim. Change*, *3*, 654–665, doi:10.1038/nclimate1845.

McAuley, S. D., J. L. Barringer, G. N. Paulachok, J. S. Clark, and O. S. Zapecza (2001), Groundwater flow and quality in the Atlantic City 800-foot sand, New Jersey, New Jersey Geological Survey Report GSR 41, 86 pp., New Jersey Department of Environmental Protection, Trenton, NJ. [Available at http://nj.usgs.gov/special/mod_maint/info/info_acty.html.]

McHutchon, A., and C. E. Rasmussen (2011), Gaussian process training with input noise, in: Advances in Neural Information Processing Systems 24, Edited by J. Shawe-Taylor et al., 1341–1349. [Available at http://books.nips.cc/papers/files/nips24/NIPS2011_0780.pdf.]

Meehl, G. A., et al. (2007), Global climate projections, in *Climate Change 2007: The Physical Science Basis*, edited by S. Solomon, D. Qin, M. Manning, Z. Chen, M. Marquis, K. B. Averyt, M. Tignor, and H. L. Miller , pp. 747–845 , Cambridge Univ. Press, New York.

Miller, K. G., M. A. Kominz, J. V. Browning, J. D. Wright, G. S. Mountain, M. E. Katz, P. J. Sugarman, B. S. Cramer, N. Christie-Blick, and S. F. Pekar (2005), The Phanerozoic record of global sea-level change, *Science*, *310*, 1293–1298, doi:10.1126/science.1116412.

Miller, K. G., P. J. Sugarman, J. V. Browning, B. P. Horton, A. Stanley, A. Kahn, J. Uptegrove, and M. Aucott (2009), Sea-level rise in New Jersey over the past 5000 years: Implications to anthropogenic changes, *Global Planet. Change*, *66*(1–2), 10–18, doi:10.1016/j.gloplacha.2008.03.008.

Milne, G. A., W. R. Gehrels, C. W. Hughes, and M. E. Tamisiea (2009), Identifying the causes of sea-level change, *Nat. Geosci.*, *2*, 471–478, doi:10.1038/ngeo544.

Minard, J. (1969), Geology of the Sandy Hook quadrangle in Monmouth County, New Jersey, *U.S. Geol. Surv. Bull., 1276*, 43 pp.

Mitrovica, J. X., and G. A. Milne (2003), On post-glacial sea level: I. General theory, *Geophys. J. Int.*, *154*, 253–267, doi:10.1046/j.1365-246x.2001.01550.x.

Mitrovica, J. X., G. A. Milne, and J. L. Davis (2001), Glacial isostatic adjustment on a rotating earth, *Geophys. J. Int.*, *147*, 562–578.

Mitrovica, J. X., N. Gomez, E. Morrow, C. Hay, K. Latychev, and M. E. Tamisiea (2011), On the robustness of predictions of sea level fingerprints, *Geophys. J. Int.*, *187*, 729–742.

National Research Council (2012), Sea-level rise for the coast of California, Oregon, and Washington: Past, present, and future, 201 pp, The National Academy Press, Washington, D. C.

Nerem, R. S., D. P. Chambers, C. Choe, and G. T. Mitchum (2010), Estimating mean sea-level change from the TOPEX and Jason Altimeter Missions, *Mar. Geodesy*, *33*, 435–446, doi:10.1080/01490419.2010.491031.

Pardaens, A. K., J. M. Gregory, and J. A. Lowe (2011), A model study of factors influencing projected changes in regional sea level over the 21st century, *Clim. Dyn.*, *36*, 2015–2033, doi:10.1007/s00382-009-0738-x.

Parris, A., P. Bromirski, V. Burkett, D. Cayan, M. Culver, J. Hall, R. Horton, K. Knuuti, R. Moss, J. Obeysekera, A. Sallenger, and J. Weiss (2012), Global sea level rise scenarios for the US National Climate Assessment, *NOAA Tech Memo OAR CPO-1*, 37 pp.

Peltier, W. R. (2004), Global glacial isostasy and the surface of the ice-age earth: The ICE-5G (VM2) model and GRACE, *Annu. Rev. Earth Planet. Sci.*, *32*, 111–149.

Pfeffer, W. T., J. T. Harper, and S. O'Neel (2008), Kinematic constraints on glacier contributions to 21st-century sea-level rise, *Science*, *321*, 1340–1343, doi:10.1126/science.1159099.

Pope, J. B., and T. J. Burbey (2004), Multiple-aquifer characterization from single borehole extensometer records, *Ground Water*, *42*, 45–58, doi:10.1111/j.1745-6584.2004.tb02449.x.

Psuty, N. P. (1986), Holocene sea level in New Jersey, *Phys. Geog.*, *7*, 156–167.

Rahmstorf, S. (2007), A semi-empirical approach to projecting future sea-level rise, *Science*, *315*, 368–370, doi:10.1126/science.1135456.

Rahmstorf, S., G. Foster, and A. Cazenave (2012), Comparing climate projections to observations up to 2011, *Environ. Res. Lett.*, *7*, 044035, doi:10.1088/1748-9326/7/4/044035.

Rignot, E., I. Velicogna, M. R. van den Broeke, A. Monaghan, and J. Lenaerts (2011), Acceleration of the contribution of the Greenland and Antarctic ice sheets to sea-level rise, *Geophys. Res. Lett.*, *38*, L05503, doi:10.1029/2011GL046583.

Sallenger, A. H., Jr., K. S. Doran, and P. A. Howd (2012), Hotspot of accelerated sea-level rise on the Atlantic Coast of North America, *Nat. Clim. Change*, *2*, 884–888, doi:10.1038/nclimate1597.

Schaeffer, M., W. Hare, S. Rahmstorf, and M. Vermeer (2012), Long-term sea-level rise implied by 1.5°C and 2°C warming levels, *Nat. Clim. Change*, *2*, 867–870, doi:10.1038/nclimate1584.

Shepherd, A., et al. (2012), A reconciled estimate of ice-sheet mass balance, *Science*, *338*, 1183–1189, doi:10.1126/science.1228102.

Sriver, R. L., N. M. Urban, R. Olson, and K. Keller (2012), Toward a physically plausible upper bound of sea-level rise projections, *Clim. Change*, *115*, 893–902.

Stanford, J. D., E. J. Rohling, S. E. Hunter, A. P. Roberts, S. O. Rasmussen, E. Bard, J. McManus, and R. G. Fairbanks (2006), Timing of meltwater pulse 1a and climate responses to meltwater injections, *Paleoceanography*, *21*, PA4103, doi:10.1029/2006PA001340.

Stanford, S. D., G. M. Ashley, E. W. B. Russell, and G. J. Brenner (2002), Rates and patterns of late Cenozoic denudation in the northernmost Atlantic Coastal Plain and Piedmont, *Geol. Soc. Am. Bull.*, *114*, 1422–1437, doi:10.1130/0016-7606(2002)114<1422:RAPOLC>2.0.CO.

Sun, H., D. Grandstaff, and R. Shagam (1999), Land subsidence due to groundwater withdrawal: Potential damage of subsidence and sea level rise in southern New Jersey, USA, *Environ. Geol.*, *37*, 290–296.

Tebaldi, C., B. H. Strauss, and C. E. Zervas (2012), Modeling sea level rise impacts on storm surges along US coasts, *Environ. Res. Lett.*, *7*, 014032, doi:10.1088/1748-9326/7/1/014032.

U.S. Census Bureau (2013), U.S. Summary: 2010 Census, US Profile, Washington, D. C.

Watts, A. B. and S. M. Steckler (1979), Subsidence and eustasy at the continental margin of eastern North America, in Talwani, M., Hay, W., and Ryan, W.B.F., eds., *Deep Drilling Results in the Atlantic Ocean: Continental Margins and Paleoenvironment*, Maurice Ewing Series 3, AGU, Washington, D. C. pp. 218–234, doi:10.1029/ME003p0218.

Yin, J., M. E. Schlesinger, and R. J. Stouffer (2009), Model projections of rapid sea-level rise on the northeast coast of the United States, *Nat. Geosci.*, *2*, 262–266, doi:10.1038/ngeo462.

Yu, S.-Y., T. E. Törnqvist, and P. Hu (2012), Quantifying Holocene lithospheric subsidence rates underneath the Mississippi Delta, *Earth Planet. Sci. Lett.*, *331–332*, 21–30, doi:10.1016/j.epsl.2012.02.021.

Zervas, C. E. (2005), Response of extreme storm tide levels to long-term sea level change, Oceans, *Proceedings of MTS/IEEE*, 2005, 2501–2506.